How Many Water Molecules Are Actively Involved in the Neutral Hydration of Carbon Dioxide?

Minh Tho Nguyen,* Greet Raspoet, and Luc G. Vanquickenborne

University of Leuven, Department of Chemistry, Celestijnenlaan 200F, B-3001 Leuven, Belgium

Piet Th. Van Duijnen

Department of Organic and Molecular Inorganic Chemistry, University of Groningen, Nijenborgh 4, NL-9747 AG Groningen, The Netherlands

Received: January 7, 1997; In Final Form: May 23, 1997[⊗]

The detailed reaction pathways for the hydration of carbon dioxide by water and water clusters containing two, three, and four water molecules ($CO_2 + nH_2O \rightarrow H_2CO_3 + (n-1)H_2O$, $n = 1-4$) have been investigated in both gas phase and aqueous solution using ab initio molecular orbital (MO) theory up to the quadratic configuration interaction QCISD(T)/6-31G(d,p)//MP2/6-31G(d,p) level, both SCRF and PCM models of continuum theory, and a mixed approach based on MO calculations in conjunction with Monte Carlo and reaction field simulations. It is confirmed that the CO_2 hydration constitutes a case of active solvent catalysis where solvent molecules actively participate as a catalyst in the chemical process. In aqueous solution the hydration mechanism is multimolecular, where geometric parameters of the solvent fully intervene in the reaction coordinate. The hydration reaction was found to proceed through an attack of a water oxygen to the CO_2 carbon in concert with a proton transfer to a CO_2 oxygen. The proton transfer is assisted by a chain of water molecules, which is necessary for a proton relay between different oxygens. Owing to a significantly larger charge separation in the transition structures, nonspecific electrostatic interactions between solute and solvent continuum also play a more important stabilizing role. Regarding the answer to the title question, our calculations suggest that although a water tetramer ($n = 4$) seems to be necessary for CO_2 hydration in the gaseous phase, a reaction channel involving formation of a bridge containing three water molecules ($n = 3$) is likely to be actively involved in the neutral hydration of CO_2 in aqueous solution.

Introduction

The hydration of carbon dioxide and its reverse, the dehydration of bicarbonate ion, are among the most fundamental reactions in several biological and environmental processes.[1] Results obtained over the past half century have shown that, in neutral aqueous solution and without the presence of enzyme, the hydration of CO_2 is subject to catalysis by the solvent. However, the question concerning the actual number of participating water molecules in the hydration/dehydration mechanism, and thereby the nature of the solvent catalytic effect, remains a matter of discussion. Let us first summarize succinctly the main results reported in the abundant literature.

For a long period, carbonic acid had not been detected by any spectroscopic means, and its formation was only inferred from kinetic data.[2−5] The first-order rate constant for CO_2 hydration was measured and falls in the range 2×10^{-2} to 5×10^{-2} s^{-1} in neutral aqueous solution (pH = 7) at room temperature; a corresponding activation energy of 74 kJ mol^{-1} could also be derived.[3] The isotope effects obtained for the hydration reaction, $k(H_2O)/k(D_2O) = 1.8$ (ref 4), $k(^{12}C)/k(^{13}C) = 1.0069$ (ref 5), are compatible with either a general base or a concerted cyclic mechanism involving at least two water molecules. Recently, the existence of carbonic acid as a stable discrete species has been demonstrated in the gas phase by neutralization−reionization mass spectroscopic techniques,[6] in acidic solution by ^{13}C NMR measurements,[7] and in vitreous methanol films at low temperature (150 K)[8a] as well as in an ice matrix[8b] both by infrared spectrometry. Molecular orbital calculations[9] of harmonic vibrational wavenumbers appear to support both IR experimental observations.

From a theoretical point of view, several studies have been available on the hydration pathways and its product.[9−21] Earlier ab initio studies showed a large discrepancy between calculated and experimental values for activation energies, and therefore, the difference in reactivities was suggested to be due to solvation effects. Although the idea of a second water molecule acting as a catalyst in the reaction process was already advanced in several earlier experimental papers,[4] it was not pursued any further by theoretical studies at that time. In 1984, Nguyen and Ha[16] demonstrated the catalytic role of an additional water molecule in the CO_2 hydration. By use of HF calculations with the small 3-21G basis set, involvement of a water dimer was shown to reduce appreciably the activation energy through a cyclic six-membered transition structure. In such a mechanism the second water molecule plays the role of a bifunctional acid−base catalyst facilitating the proton transfer. Subsequently, the catalytic effect was confirmed by MO calculations using larger basis sets including polarization functions (6-31G** and larger sets)[18−20] and electron correlation via Møller−Plesset perturbation theory (MP*n*), but the refined energetic data turned out to disagree with experimental results, at least as far as activation parameters are concerned. The higher the level of theory, the more substantial the barrier height.

More recently, Merz[20] performed free energy perturbation calculations in conjunction with both molecular dynamics and Monte Carlo simulations to address the influence of solvation energy on the CO_2 hydration. This author[20] found again that the two-water reaction is in better agreement with experimental results than the one-water reaction and suggested that the former should be the dominant process in aqueous solution. Note that not only studies on carbon dioxide have predicted such a barrier

[⊗] Abstract published in *Advance ACS Abstracts,* September 1, 1997.

S1089-5639(97)00104-7 CCC: $14.00

decrease by active participation of an assistant water molecule. Several authors have found a similar behavior in the hydration of ketene−imine,[22] ketene,[23] or formaldehyde.[24] Recently, the formaldehyde hydration has been reinvestigated by Wolfe et al.[25] introducing four water molecules in which the hydration is catalyzed by a bridge of three additional water molecules. These authors[25] argued that multiple water molecules should be considered to adequately model a hydrolytic process.

In an attempt to obtain more insight into this important problem, we have performed a series of calculations to probe further the influence of aqueous solution on the CO_2 hydration. For this purpose, two different strategies are used to approach the solvation phenomenon. Both strategies differ from each other essentially in the solvent description. On the one hand, the solvent is considered as a macroscopic and continuous medium and the solute−solvent electrostatic interaction is taken into account. On the other hand, the microscopic representation of a discrete number of solvent molecules is explicitly considered. Although the solute is always treated quantum mechanically, there are two possibilities for simulating the solvent, namely, (i) a full quantum mechanical treatment within the framework of the supermolecule approach and (ii) a classical representation with the aid of a Monte Carlo simulation. The supermolecule approach (i) gives no doubt a more rigorous description of the solute−solvent interaction, but owing to the high cost of the actual calculation, only a very limited number of solvent molecules can be included. In the present theoretical study, we have focused our attention on the specific interactions of solvent molecules for which up to four participating water molecules have been considered. The use of classical mechanics to mimic the solvent in (ii) is performed by using Monte Carlo calculations and is incorporated in a combined model[27] in which both discrete and continuum representations were accounted for simultaneously. In this regard, the present approach is comparable to that of Merz,[20] but the number of active water molecules taken into consideration is larger and the treatment of the continuum solvation is different. Because a significant charge separation in the solute was found during the catalyzed process, the passive, electrostatic influences of the surrounding medium are expected to play an important role depending on the solvent polarity. It should also be stressed that the hydration of carbon dioxide can serve as a basic model for the investigation of general mechanistic features of this class of reaction, including various topics such as solvation, modes of solvent catalysis, and the relationships between structural variables and charge distributions in transition states. The conclusions obtained in the present paper also help in understanding the hydrolysis of analogous systems such as carbonyl and cumulene compounds.

Methods and Calculations

Ab initio molecular orbital calculations were carried out using the GAUSSIAN 94 set of programs.[26] The stationary points of interest were initially located and characterized by harmonic vibrational analysis employing Hartree−Fock (HF) calculations with the dp-polarized 6-31G(d,p) basis set. The relevant structures were then reoptimized at the second-order Møller−Plesset perturbation theory (MP2) level with the same basis set. Improved relative energies between stationary points were finally estimated using the quadratic configuration interaction method (QCISD(T)) with the 6-31G(d,p) basis at MP2/6-31G(d,p) optimized geometries. These relative values were also corrected for zero-point vibrational energies (ZPE) derived from HF/6-31G(d,p) calculations and scaled by 0.9.

The understanding of the effect of solvation on reaction rates has been tackled by employing different approaches. We initially assembled the reacting sphere using the supermolecule approach in which the solvent molecules are considered explicitly. The sphere is constituted of a carbon dioxide molecule and some reacting water molecules (up to four molecules), and quantum chemical calculations are performed for the whole system. All structures of interest were treated at the same level of theory. A complete treatment of solvation effects needs to include not only the influence of the active region of the solvent, whose structure is modified by the presence of the solute, but also that of the bulk solvent. For the latter purpose, the solvent is represented by an infinite dielectric and polarizable continuum characterized by its dielectric constant (ϵ). In the present paper, different techniques have been applied. First, we used the Onsager self-consistent reaction field method (SCRF), in which the electrostatic expansion is truncated at the dipole level and a spherical cavity is used. All relevant gas-phase stationary structures were reoptimized in water solution ($\epsilon = 78.3$) using this approach at the HF(SCRF)/6-31G(d,p) level. Furthermore, single-point calculations were done including electron correlation (MP2) using both 6-31G(d,p) and 6-311++G(d,p) basis sets. Second, the polarizable continuum model (PCM) developed by Tomasi and co-workers[27a] was also applied. Although the latter constitutes a more realistic method than the former by using a cavity that adapts to the molecular shape instead of a sphere, only single-point calculations could be performed up to the MP2(PCM)/6-31G(d,p) level. Owing to the lack of analytic gradients, full geometry optimizations using PCM cannot be achieved.

Third, the direct reaction field (DRF) method by Van Duijnen et al.[27b] was also used. This treatment is based on the use of a molecular-shaped algorithm to define the solute−solvent interface and a numerical solution of the Poisson equation, using in addition a more rigorous expression of the molecular electrostatic potential. Finally, solvent influences were simulated by a combined (discrete + continuum) model. The supermolecule of interest is treated quantum mechanically. Subsequently, a number of subsystems have been defined and are treated in a discrete classical way by a Monte Carlo simulation. The "quantum + discrete classical" system is enveloped by a surface, defining the boundary between both discrete and continuum systems. The system outside the boundary is modeled by the DRF continuum theory. All computations for the DRF as well as the combined model were performed at the HF level with a DZP basis set.

Results and Discussion

In Vacuum Reaction Pathways Using Supermolecule Approach. The reaction pathways for both $CO_2 + nH_2O \rightarrow H_2CO_3 + (n-1)H_2O$ reactions with $n = 1$ and 2 have already been calculated at the Hartree−Fock level using various small and medium basis sets.[16−20] We now recompute these paths using correlated wave functions including larger basis sets. Furthermore, we examine how the potential energy curve is modified when CO_2 interacts with a larger chain of water molecules, namely, $n = 3$ and 4. Tables 1 and 2 show the total, zero-point, and relative energies of all structures calculated for the mechanism in vacuum. Selected optimized parameters for the reactant complex, transition structure, and product complex for each of the four hydration pathways of carbon dioxide ($CO_2 + nH_2O \rightarrow H_2CO_3 + (n-1)H_2O$, $n = 1$, 2, 3, and 4) are displayed in Figures 1−4. For the sake of convenience and comparison, the geometries in the solvent continuum are also given, but they will be discussed in a following section. The bond lengths and bond angles shown for these structures refer to both HF/6-31G(d,p) and MP2/6-31G(d,p) optimizations in the gas phase ($\epsilon = 1$) and HF(SCRF)/6-31G(d,p) optimization

TABLE 1: Calculated Total (hartree) and Zero-Point Vibrational (ZPE, kJ mol^{-1}) Energies for the Hydrolysis of Carbon Dioxide ($CO_2 + nH_2O \rightarrow H_2CO_3 + (n-1)H_2O$; $n = 1-4$)

	HF[a] 6-31G**	MP2[b] 6-31G**	MP2[b] 6-311++G**	QCISD(T)[b] 6-31G**	ZPE[c]
CO_2	−187.634 18	−188.118 36	−188.206 28	−188.122 90	30
H_2O	−76.023 61	−76.222 45	−76.274 91	−76.231 65	55
$CO_2 + H_2O$	−263.657 79	−264.340 81	−264.481 19	−264.354 55	85
$CO_2\cdots H_2O$ **R1**	−263.663 00	−264.346 60	−264.485 76	−264.360 33	88
TS **TS1**	−263.559 92	−264.265 06	−264.397 87	−264.278 18	86
H_2CO_3 **P1**	−263.657 03	−264.331 85	−264.464 09	−264.348 85	103
$CO_2 + 2H_2O$	−339.681 40	−340.563 26	−340.756 10	−340.586 20	140
$CO_2\cdots 2H_2O$ **R2**	−339.699 01	−340.585 63	−340.772 84	−340.607 91	153
TS **TS2**	−339.631 21	−340.534 98	−340.713 81	−340.555 95	153
$H_2CO_3\cdots H_2O$ **P2**	−339.695 07	−340.573 91	−340.753 73	−340.599 12	165
$H_2CO_3 + H_2O$	−339.680 64	−340.554 30	−340.739 00	−340.580 50	158
$CO_2 + 3H_2O$	−415.705 01	−416.785 71	−417.031 01	−416.817 85	195
$CO_2\cdots 3H_2O$ **R3**	−415.737 23	−416.812 03	−417.064 53	−416.861 29	217
TS **TS3**	−415.678 43	−416.764 71	−417.010 94	−416.812 43	221
$H_2CO_3\cdots 2H_2O$ **P3**	−415.732 54	−416.815 86	−417.044 28	−416.849 03	229
$H_2CO_3 + 2H_2O$	−415.704 25	−416.776 75	−417.013 91	−416.812 15	213
$CO_2 + 4H_2O$	−491.728 62	−493.008 16	−493.305 92		250
$CO_2\cdots 4H_2O$ **R4**	−491.779 57	−493.053 32	−493.358 58		284
TS **TS4**	−491.724 98	−493.013 65	−493.306 84		282
$H_2CO_3\cdots 3H_2O$ **P4**	−491.770 55	−493.035 24	−493.335 75		293
$H_2CO_3 + 3H_2O$	−491.727 86	−492.999 20	−493.288 82		266

[a] Based on HF/6-31G(d,p) geometries. [b] Based on MP2/6-31G(d,p) geometries. [c] Zero-point energies from HF/6-31G(d,p) and scaled by 0.9.

TABLE 2: Calculated Relative Energies (kJ mol^{-1}) for the Hydrolysis Pathways of Carbon Dioxide, All Corrected by Zero-Point Energies

	HF[a] 6-31G**	HF[a] 6-31G**	MP2[b] 6-311++G**	QCISD(T)[b] 6-31G**
$CO_2 + H_2O$	0	0	0	0
$CO_2\cdots H_2O$ **R1**	−11	−12	−9	−12
TS **TS1**	258	200	220	202
H_2CO_3 **P1**	20	41	63	33
$CO_2 + 2H_2O$	0	0	0	0
$CO_2\cdots 2H_2O$ **R2**	−33	−45	−31	−44
TS **TS2**	145	87	124	92
$H_2CO_3\cdots H_2O$ **P2**	−11	−3	31	−9
$H_2CO_3 + H_2O$	20	41	63	33
$CO_2 + 3H_2O$	0	0	0	0
$CO_2\cdots 3H_2O$ **R3**	−62	−47	−66	−92
TS **TS3**	96	82	79	41
$H_2CO_3\cdots 2H_2O$ **P3**	−38	−45	0	−47
$H_2CO_3 + 2H_2O$	20	41	63	33
$CO_2 + 4H_2O$	0	0	0	
$CO_2\cdots 4H_2O$ **R4**	−99	−84	−104	
TS **TS4**	42	48	30	
$H_2CO_3\cdots 3H_2O$ **P4**	−67	−28	−34	
$H_2CO_3 + 3H_2O$	20	41	63	

[a] Based on HF/6-31G(d,p) geometries. [b] Based on MP2/6-31G(d,p) geometries.

in aqueous solution ($\epsilon = 78.3$). In general, the letters **R***n*, **TS***n*, and **P***n* refer to the reactant complex, transition structure, and product complex, respectively, with $n = 1-4$ water molecules. Unless otherwise noted, we will employ the best relative energies available obtained from QCISD(T)/6-31G(d,p) + ZPE calculations in the following discussion for $n = 1-3$.

n = 1. The uncatalyzed path has been investigated by different groups.[11,16−20] It seems, however, necessary to describe again the main features. A significant feature of the transition structure **TS1** is the presence of an essentially planar four-membered ring formed between the O−H bond of the attacking water and the C−O bond of carbon dioxide (Figure 1). The water is oriented in such a way that one of its lone pairs aligns approximately along the newly forming O−C bond. In the vibrational mode corresponding to the imaginary frequency ($\nu = 2137$i cm^{-1}), the dominant motion involves the endocyclic proton, which is being transferred between both oxygen atoms, and that of the carbon atom, which is moving toward the nucleophilic water oxygen. As shown in Table 3, addition of diffuse functions to the 6-31G(d,p) basis set actually increases the activation energy in contrast to the correlation

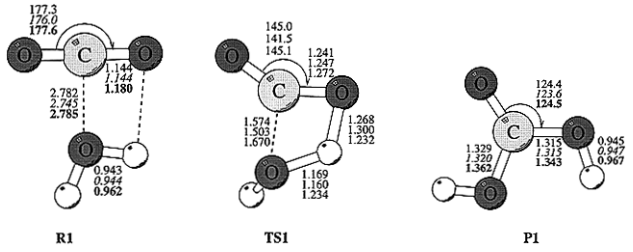

Figure 1. Optimized structures of reactant complex **R1**, transition structure **TS1**, and product complex **P1** for the reaction of carbon dioxide with one water molecule ($CO_2 + nH_2O \rightarrow H_2CO_3$, $n = 1$). HF/6-31G(d,p) parameters; HF/SCRF/6-31G(d,p) parameters; MP2/6-31G(d,p) parameters.

TABLE 3: Energy Barriers (kJ mol^{-1}) for the Hydrolyses of Carbon Dioxide, Including Different Numbers of Solvent Molecules

	HF[a] 6-31G**	MP2[b] 6-31G**	MP2[b] 6-311++G**	QCISD(T)[b] 6-31G**
$CO_2 + 1H_2O$	268	213	229	214
$CO_2 + 2H_2O$	178	133	155	136
$CO_2 + 3H_2O$	159	128	144	132
$CO_2 + 4H_2O$	141	131	134	

[a] Based on HF/6-31G(d,p) geometries. [b] Based on MP2/6-31G(d,p) geometries. All parameters are relative to the reactant complexes.

effect, which lowers the activation energy at every level. Relative to the complex **R1**, the energy barrier for the reaction $H_2O + CO_2 \rightarrow H_2CO_3$ amounts to 229 kJ mol^{-1}. This value differs somewhat from the previous ones obtained from lower level calculations, but it remains much higher than the activation energy of 74 kJ mol^{-1} experimentally determined in aqueous solution.[2]

Our calculations confirm that the hydration is endothermic by 63 kJ mol^{-1}, a value slightly larger than the earlier theoretical value of 43 kJ mol^{-1} reported in ref 9. In any case, carbonic acid is less stable than the separated $CO_2 + H_2O$ species. On the other hand, the reactant complex **R1** having a T-form is rather weak, having a complexation energy of −9 kJ mol^{-1}. In an earlier thermochemical study of the CO_2-H_2O system,[28] an enthalpy of reaction of −20 kJ mol^{-1} has been derived. It is thus obvious that the product detected in that experimental study[28] corresponds to the complex **R1** rather than to carbonic acid **P1**. Existence of a van der Waals complex **R1** has also

been demonstrated by different IR studies either in a matrix[29−30] or in solution,[31] as well as in the gas phase by microwave study.[32] Characteristics of this complex have been established in recent theoretical studies.[33]

For the $H_2CO_3 \rightarrow CO_2 + H_2O$ reaction, the energy barrier to decomposition amounts to 169 kJ mol^{-1} via **TS1**, a value consistent with the fact that carbonic acid does survive during the neutralization−reionization mass spectrometric experiment.[6]

n = 2. Figure 2 shows MP2/6-31G(d,p) optimized parameters related to the addition of a water dimer to carbon dioxide. This pathway has been abundantly commented in earlier theoretical papers.[16,18−20] For the sake of comparison, let us again recall briefly some important features. Along this path, an initial association of two water molecules with carbon dioxide results in a cyclic complex **R2** stabilized by 31 kJ mol^{-1} relative to the three separated species. This complex then proceeds across a barrier of 155 kJ mol^{-1} through transition structure **TS2**, giving a complex **P2** associating both H_2CO_3 and H_2O. The difference in energy barriers between both pathways via **TS1** and **TS2** is thus about 74 kJ mol^{-1} (229−155 kJ mol^{-1}, Table 3). The magnitude of such a reduction indicates a significant positive catalysis actually induced from the addition of a second water molecule. Essentially, this reduction in energy forms the basis for an active catalytic effect of solvent molecules put forward in earlier studies.[16]

The atoms involved in the making and breaking O−C and O−H bonds form a compact six-membered ring, which ensures a continuous hydrogen-bonded chain. As shown in Figure 2, the O−H−O−H sequence of the water dimer in **TS2** is nearly coplanar; the carbon also lies in this plane. The two hydrogen bonds (O−H−O) form an angle of about 155°, and it is presumed that their near-linearity subjects the ring to a reduced strain, which can be, in addition, best accommodated by a coplanar arrangement of the atoms involved. The exocyclic hydrogen atoms are staggered with respect to each other, thereby minimizing steric repulsion and allowing for optimal interaction of the lone-pair electrons on the attacking oxygen with the vacant Π* orbital of the carbonyl group. When the geometrical parameters of both **R2** and **TS2** are compared, it may be noted that ring deformation is substantial. The intermolecular C···O and O···H distances between CO_2 and the water dimer become, respectively, 0.734 and 0.432 Å shorter in **TS2**, indicating a more compact transition state.

The imaginary vibrational frequency becomes smaller (ν_i = 1163i cm^{-1}). The transition vector associated with the imaginary normal mode is displayed in ν_i (**TS2**).

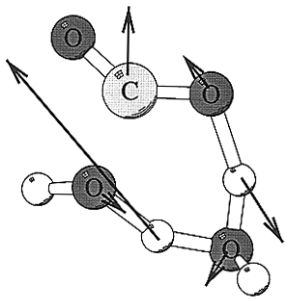

ν_i (**TS2**)

The variation of entropy amounts to $\Delta S^{\#} = -284$ J mol^{-1} K^{-1} (Table 5). The most important motion involves the water dimer in which one intermolecular distance shortens while the other lengthens; the HOH angles in both water monomers become 14.4° and 23.5° larger in **TS2** than in **R2**. In other words, migration of the hydrogen atom between both oxygen atoms is already well advanced in **TS2**. It is beyond doubt that such a transfer motion creating a charge separation can be better stabilized within the dimer. The hydrogen transfer to CO_2 oxygen is assisted by, or in concert with, another transfer within the water dimer. Such a proton relay constitutes the basis of a bifunctional acid−base catalytic action. At this stage, there is, however, no indication of any zwitterionic intermediate. The path is concerted with a single transition state **TS2**.

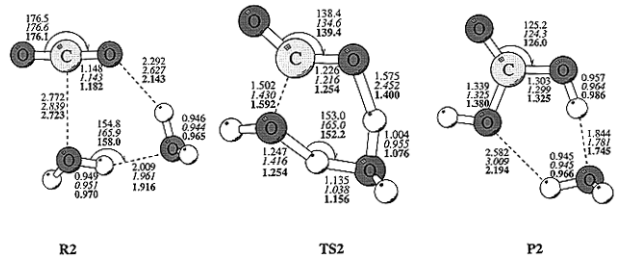

R2 **TS2** **P2**

Figure 2. Optimized structures of reactant complex **R2**, transition structure **TS2**, and product complex **P2** for the reaction of carbon dioxide with two water molecules ($CO_2 + 2H_2O \rightarrow H_2CO_3 + H_2O$). HF/6-31G(d,p) parameters; HF/SCRF/6-31G(d,p) parameters; MP2/6-31G(d,p) parameters.

Table 3 indicates that it is unlikely that any substantial fraction of the actual gas-phase hydration of carbon dioxide passes through **TS1** owing to its large activation energy. Although introduction of a single assistant water molecule to form **TS2** yields a reduction of 74 kJ mol^{-1} in the activation energy, as mentioned above, the calculated value remains too large compared with the experimental value (74 kJ mol^{-1}). Thus, the question arises as to whether introduction of even more water molecules in the supermolecule may stabilize the transition state further to catalyze the hydration reaction sufficiently. Apparently, **TS2** still contains a certain amount of strain in its cyclic structure. This strain might be relieved by incorporation of additional water molecules into the hydrogen-bonded chain. The question of interest concerns thus the smallest number of participating water molecules required in order to "bridge the gap" between gas-phase and solution behavior in carbon dioxide hydration. In what follows, we will examine, for the first time, the reaction pathways incorporating three and four water molecules.

n = 3. Calculations involving three water molecules, summarized in Figure 3 and Table 3, show again that a preassociation mechanism occurs in which an attacking oxygen approaches the central carbon whereas the water chain bridges the hydrogens to place one of them in front of a CO_2 oxygen. Starting from the reactant complex **R3**, the concerted attack of water chain leads to an eight-membered ring **TS3** whose identity is confirmed by the normal mode of the imaginary vibrational frequency (ν = 299i cm^{-1}) displayed in ν_i (**TS3**). The energy

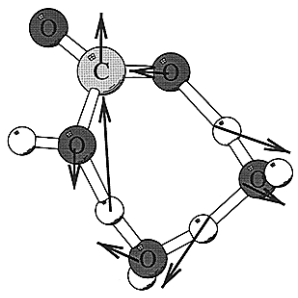

ν_i (**TS3**)

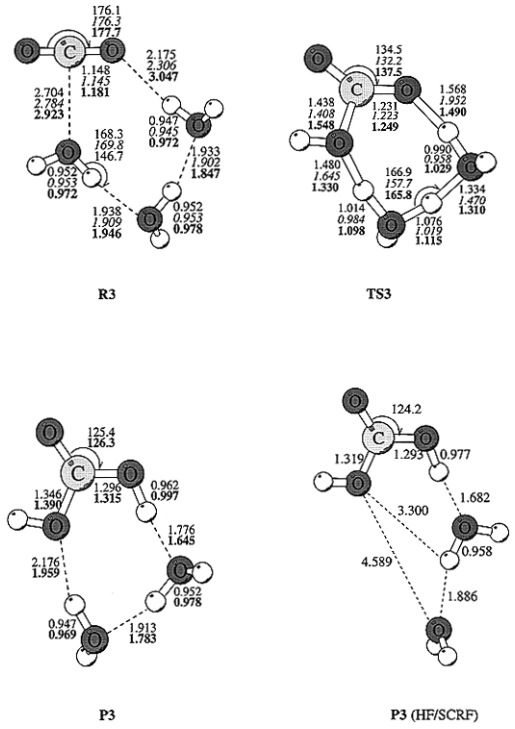

Figure 3. Optimized structures of reactant complex **R3**, transition structure **TS3**, and product complex **P3** for the reaction of carbon dioxide with three water molecules ($CO_2 + 3H_2O \rightarrow H_2CO_3 + 2H_2O$). HF/6-31G(d,p) parameters; HF/SCRF-6/31(d,p) parameters; MP2/6-31G(d,p) parameters.

barrier is calculated to be 144 kJ mol^{-1} relative to **R3**, which is lowered by 85 kJ mol^{-1} with respect to the uncatalyzed reaction ($n = 1$) but only 11 kJ mol^{-1} relative to the process with water dimer ($n = 2$). The hydrogen bonding in cyclic structures such as **R3** and **TS3**, as shown in Figure 3, may be better accommodated with proton donor−acceptor arrangements, and the considered angles are even closer to linearity than in **R2** and **TS2**.

In general, in a large molecule, hydrogen bonds of the type X−H···Y are independent of each other and their attractive forces are approximately additive. However, as in a O−H group, if the donor O−H is simultaneously an acceptor and if several of these groups associate, O−H···O−H···O−H···, a cooperative phenomenon comes into play.[34] Usually, the cooperative phenomenon is understood as an increase in the stability of hydrogen bonds, which is attributed to a mutual polarization of the associated O−H groups. This means that permanent multipoles of one water molecule polarize the electron clouds of the second and then the third and fourth molecules, etc., which results finally in a greater attraction between them. One of the consequences of such cooperativity is the elongation of the donor O−H bonds upon formation of an O−H···O hydrogen bond. This phenomenon increases the polarization of the bonds and results in an improved hydrogen-bonding interaction energy. On the other hand, this increase renders the monomers somewhat less stable. The final energy balance will therefore depend on the mutual polarization of the hydrogen bonds. The transition structure **TS3** involves a cyclic system of eight atoms apparently satisfying the preferred requirement for intramolecular proton transfer as postulated by Gandour.[35] Accordingly, the highest probability for intramolecular proton transfer occurs when a cyclic transition state can accommodate a linear arrangement of proton-donor−acceptor of appropriate length. In fact, this occurs more easily when the ring size contains eight atoms as in **TS3** rather than six as in **TS2**. Nevertheless, the relative importance of linear versus nonlinear transfer and of the involvement of a hydroxylic molecular bridge (i.e. a second water molecule) in determining a possible mechanism is not obvious. In this case, there is no convincing evidence that one single factor is dominant, even though as indicated from numerous theoretical studies for pure hydrogen bonds, a linear arrangement of proton-donor−acceptor is energetically more favorable than a nonlinear arrangement. In view of the small reduction of only 11 kJ mol^{-1} in the energy barrier in going from **TS2** to **TS3**, it can be suggested that when intermolecular proton transfer occurs, a cyclic transition state having an adequate size to accommodate linear arrangements is a necessary but not a sufficient condition.

As seen in Figures 2 and 3, the presence of a bicarbonate [HCO_3^-] entity interacting with a hydroxonium cation becomes more important in **TS2** and **TS3**. This can be confirmed by a comparison with the geometry of the isolated HCO_3^- ion optimized at the same level. Again, within the cationic moiety, the $H_3O^+ \cdot OH_2$ structure is virtually formed. Thus, in **TS3**, the third water molecule is divided into OH^- and H^+ without additional cost; while the hydroxyl anion is being added to CO_2 carbon, the proton is fully transferred to the water dimer. Although, within the latter, the hydrogen migration is less advanced than that in **TS2**, the water dimer still forms quite a compact entity. Performing a Mulliken population analysis at the MP2/6-31G(d,p) level offers a further probe for the detection of ionic entities: total charges on the [HCO_3^-] system in **TS2** and **TS3** amount to −0.77 and −0.68 electron, respectively. A clear charge separation can be seen in both transition structures, which is reminiscent of a zwitterionic structure. This fact is expected to be important when electrostatic solvent effects are taken into account. More details are given in the following section. Although **TS3** exhibits a zwitterionic character, intrinsic reaction coordinate (IRC) calculations indicate that there is no zwitterionic intermediate on the reaction pathway. The path remains concerted with a single transition state.

n = 4. After extensive search, we were able to locate the transition structure **TS4** made up of four water molecules. Figure 4 shows the related HF and MP2/6-31G(d,p) optimized parameters. In this case, the hydration process seems to take place by a simultaneous proton transfer to the CO_2 oxygen and an attack by a water oxygen of neutral carbon in two different planes. Some perspective views of this approach are given in the structures **TS4(a)** and **TS4(b)**. Such a transfer can only

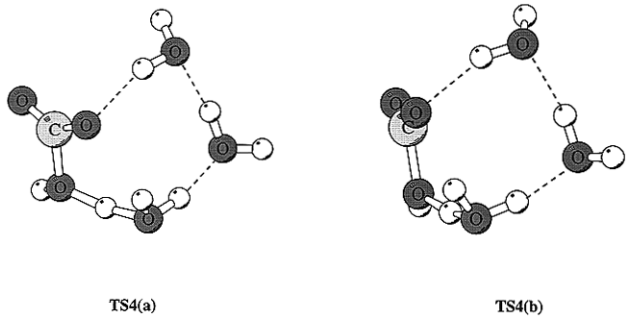

occur with the aid of several bridging water molecules.

As shown in Figure 4, a remarkable feature attributed to **TS4** is the existence of a water dimer entity, whose structure is somewhat similar to the structure in **TS3** discussed above. Again, the hydrogen transfer to CO_2 oxygen is assisted by a transfer relay essentially within a water dimer, which apparently constitutes the basis of bifunctional catalytic action. However, the dimer itself is probably too small to bridge both reacting centers, and ring strain becomes an important factor in its cyclic structure. A third or fourth solvent molecule is obviously

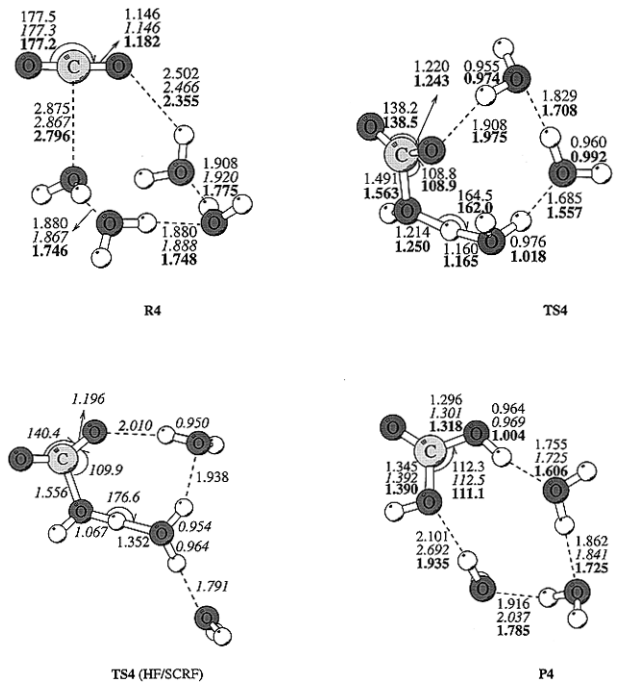

Figure 4. Optimized structures of reactant complex **R4**, transition structure **TS4**, and product complex **P4** for the reaction of carbon dioxide with four water molecules ($CO_2 + 4H_2O \rightarrow H_2CO_3 + 3H_2O$). HF/6-31G(d,p) parameters; HF/SCRF/6-31G(d,p) parameters; MP2/6-31G(d,p) parameters.

needed to bridge the gap and carry on the proton transfer in a comfortable and rapid way. However, calculated values of the activation parameters given in Table 3 show little change in the energy barrier when going from $n = 3$ to $n = 4$. As seen from a vibrational analysis of **TS4**, all protons in the cyclic H-bonded system contribute to the transition vector. No tendency could be found for the proton transfers to be uncoupled (see ν_i (**TS4**)). Again, we were not able to locate any

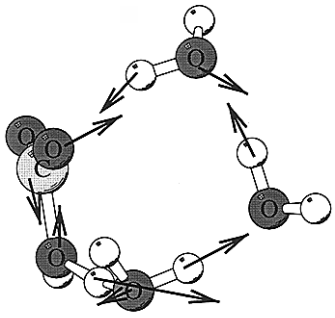

intermediate that would refer to a stepwise mechanism. It does not seem plausible that one proton transfer has become uncoupled from the other components of the reaction.

In summary, our results suggest that two ($n = 3$) or three ($n = 4$) additional water molecules are involved in the gas-phase hydration of carbon dioxide.

To understand the energetics of the catalysis, the Gibbs energy rather than the enthalpies need to be considered. Indeed, entropy effects could be less favorable for a water chain intervention than for an uncatalyzed reaction. Although calculated thermodynamic parameters for all structures considered are given in Table 4, Table 5 lists values of activation $\Delta H^{\#}$, $\Delta S^{\#}$, and $\Delta G^{\#}$ at standard conditions, including thermal corrections (0 K →

TABLE 4: Calculated Energies (kJ mol^{-1}, 0 K), Enthalpies (kJ mol^{-1}, 298 K), Entropies[a] (J mol^{-1} K^{-1}, 298 K), and Free Energies (kJ mol^{-1}, 298 K) along Both Catalyzed and Uncatalyzed Paths

	ΔE^b	$\Delta H_{298}{}^c$	ΔS	ΔG
$CO_2 + H_2O$	0	0	0	0
$CO_2\cdots H_2O$ **R1**	−11	−8	−61	10
TS **TS1**	258	254	−133	293
H_2CO_3 **P1**	20	15	−134	55
$CO_2 + 2H_2O$	0	0	0	0
$CO_2\cdots 2H_2O$ **R2**	−33	−31	−198	28
TS **TS2**	145	138	−284	222
$H_2CO_3\cdots H_2O$ **P2**	−11	−14	−246	60
$H_2CO_3 + H_2O$	20	15	−134	55
$CO_2 + 3H_2O$	0	0	0	0
$CO_2\cdots 3H_2O$ **R3**	−62	−60	−310	33
TS **TS3**	96	88	−413	211
$H_2CO_3\cdots 2H_2O$ **P3**	−38	−41	−356	65
$H_2CO_3 + 2H_2O$	20	15	−134	55
$CO_2 + 4H_2O$	0	0	0	0
$CO_2\cdots 4H_2O$ **R4**	−99	−98	−448	35
TS **TS4**	42	36	−534	195
$H_2CO_3\cdots 3H_2O$ **P4**	−67	−70	−485	75
$H_2CO_3 + 3H_2O$	20	15	−134	55

[a] Results based on HF/6-31G(d,p) geometries. [b] Including zero-point energies (all corrected by 0.9). [c] Including thermal corrections and zero-point energies (all corrected by 0.9).

TABLE 5: Enthalpy Changes (kJ mol^{-1}, 298 K), Entropy[a] Changes (J mol^{-1} K^{-1}, 298 K), and Free Energies (kJ mol^{-1}, 298 K) along Both Catalyzed and Uncatalyzed Paths in Gas Phase and in Solvent

	gas phase[b]			solvent[c]		
	$\Delta H^{\#}$ [d]	$\Delta S^{\#}$ [e]	$\Delta G^{\#}$ [e]	$\Delta H^{\#}$ [d]	$\Delta S^{\#}$ [d]	$\Delta G^{\#}$ [d]
$CO_2 + 1H_2O$	254	−133	293	248	−63	267
$CO_2 + 2H_2O$	169	−284	222	116	−92	144
$CO_2 + 3H_2O$	148	−413	211	102	−103	133
$CO_2 + 4H_2O$	134	−534	195	70	−61	87

[a] Results based on HF/6-31G(d,p) vibrational analyses. [b] Results in gas phase, based on HF/6-31G(d,p) geometries. [c] Results in solvent, based on SCRF-HF/6-31G(d,p) geometries. [d] Relative to the reactant complexes. [e] Relative to the isolated molecules.

298 K), calculated in both the gas phase and solvent. As seen in Table 4, in the gas phase, the isolated molecules ($CO_2 + nH_2O$) are thermodynamically preferred as the reactant state over the reactant complex $CO_2\cdots nH_2O$. The unfavorable entropy changes for association of the reactant complex are not compensated by the negative enthalpy change calculated. Therefore, the Gibbs energies of the respective transition structures must be compared with those of the isolated molecules. Thus, insertion of an additional water molecule into the structure of **TS1** (**TS1** + $H_2O \rightarrow$ **TS2**) reduces the free energy of activation by 71 kJ mol^{-1}. This effect arises from an unfavorable entropy change of −284 J mol^{-1} K^{-1}, consistent with a substantial restriction of mobility as the free water molecule becomes frozen into a cyclic structure, and from a more favorable enthalpy change derived from a series of factors, including bond formation, strain relief, etc. It is noted that only a transition state such as **TS2** has such a capacity for extraordinary stabilization, since the gain in enthalpy of association in both reactant and product states is insufficient to compensate the entropy cost. This model seemingly exhibits an essential property of a catalytic process, namely, a capacity for strong transition-state stabilization by a catalyst that either fails to stabilize or induces only a much smaller stabilization of the reactant and product states. An entropy difference of −121 J mol^{-1} K^{-1} between both transition structures **TS2** and **TS3** can be noted, which is due to the loss of translational and

rotational freedom of a free water molecule upon its incorporation into **TS3**. This is compensated by enthalpy gain that is basically the source of the catalytic effect. As a matter of fact, in hydrogen-bonded systems, the loss of entropy that accompanies the organization of three molecules into a preassociating complex has been found to be balanced almost exactly by the enthalpy advantage associated with increased linearity of the hydrogen transfers.[34,35] The entropy variations are not large enough in the case of the three-water molecule reaction to make it unfavorable relative to the two-water molecule reaction. Overall, the hydration reaction incorporating four water molecules (via **TS4**) occurring in the gas phase without solvent continuum influences appears to be the most favorable in terms of either enthalpies or Gibbs energies. In view of the energetic convergence in going from $n = 2$ to $n = 4$, it is expected that further incorporation of active water molecules induces only minor improvements.

Although in the gas phase energy changes are compared to the isolated molecules, in solution the cyclic reactant complex is likely to provide a reasonable approximation for the appropriate reactant state in the condensed medium. Therefore, the energy changes in the solvent reported in Table 5 are compared to those of the reactant complex, since the process is effectively unimolecular.

Reaction in Aqueous Solution Using Continuum Approach. In this section, the macroscopic influence of the solvent and its repercussion on the geometries and energetics of the process will be taken into account. First, we have considered SCRF calculations in which the previously optimized gas-phase structures were used to estimate the radius of the spherical cavities, and these values were used in subsequent HF(SCRF) optimizations. A dielectric constant of $\epsilon = 78.3$ was used to describe the water continuum. In the case of strongly polar structures such as **TS2**, **TS3**, and **TS4**, the electrostatic influence of the surrounding medium can be expected to play the most important role.

In Figures 1−4 the optimized geometry parameters of the relevant structures in aqueous solution are also summarized. All SCRF optimizations were only performed at the HF level, owing to the lack of analytical energy gradients at the MP2 level. Optimizations at the MP2(SCRF) level by calculating numerically energy gradients and Hessians are beyond our present computational resources.

It is remarkable that, when geometrical parameters of the supermolecule were relaxed in solvent using the SCRF method, a transition state containing four active waters cannot be found anymore. As shown in Figure 4, the **TS4**, in aqueous solution, contains only three water molecules forming the water chain to perform the considered hydrogen transfer; the fourth water molecule goes outside the ring, forming a hydrogen bond with a participating water. Figure 5 shows the electrostatic solvent effect for the various hydration pathways of CO_2 in solvent, computed by the classical Onsager SCRF method; the corresponding energies are recorded in Table 6. Figure 5 suggests that the solvent polarity stabilizes the transition structures **TS2** and **TS3** significantly more than it does **TS1** ($n = 1$). This difference in stabilizing effect is due to the fact that, in the transition structure without an extra water molecule **TS1**, no significant polarization occurs. Further support for this statement can be found in the geometries given in Figures 1−3. The medium apparently favors the polarity of the transition structures **TS2** and **TS3** by accentuating charge separation. The continuum tends to lengthen the intermolecular distances between the HCO_3^- entity and the H_3O^+, $H_5O_2^+$, and $H_7O_3^+$ systems, respectively, thus opening the transition states. A comparison

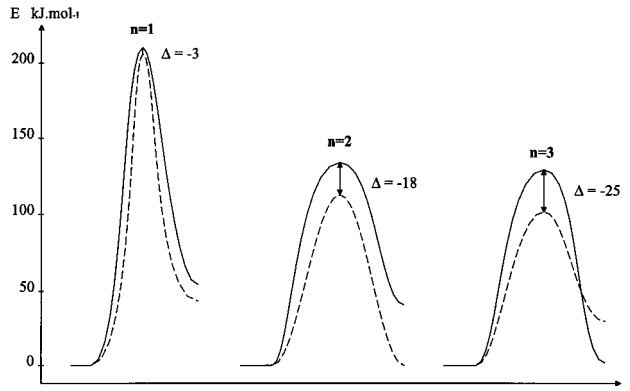

Figure 5. Electrostatic solvent effects for $CO_2 + nH_2O \rightarrow H_2CO_3 + (n-1)H_2O$ ($n = 1-3$) hydration reactions based on MP2(SCRF)/6-31G(d,p)//MP2/6-31G(d,p) calculations. Δ indicates the stabilization of the solvent reaction field compared with the gas-phase results.

of the distances are displayed in **TS2(a)** and **TS3(a)**. More

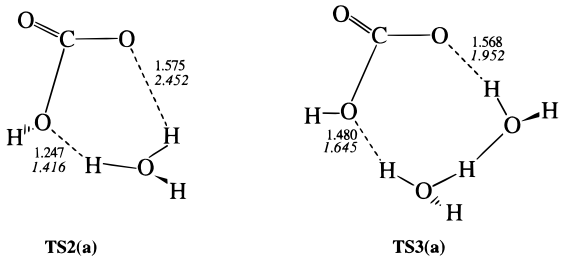

TS2(a) **TS3(a)**

Bond lengths at HF/6-31G(d,p).
Bond lengths at HF-SCRF/6-31G(d,p).

open transition states induce smaller variations of entropy, which in turn contributes positively to the reaction rates. Nevertheless, it seems difficult at this stage to view whether such lengthenings are genuine effects or just an artifact of the Onsager model using a spherical cavity.

Note that the geometry of the reactant complexes **R2**−**R3** changes only marginally in aqueous solution (see Figure 3). The H_2CO_3 product undergoes strong hydrogen bonding with only one water molecule; the other water molecules turn away from the product and do not seem to have much influence. To estimate the magnitude of the water continuum effect, SCRF calculations using the gas phase geometries have been performed. When the solvent reaction field is included, the energy barriers amount to 114 and 107 kJ mol^{-1} for $n = 2$ and 3, respectively, at the MP2(SCRF)/6-31G(d,p)//MP2/6-31G(d,p) level, which represent reductions of, respectively, 19 and 21 kJ mol^{-1} relative to the corresponding gas-phase barriers (MP2/6-31G(d,p) values). Tables 6 and 7 also contain the values that include the relaxation of the geometry in a continuum. It turns out that the MP2(SCRF)/6-311++G(d,p) results based on geometries optimized in the solvent continuum do not differ significantly from the SCRF results using gas-phase geometries for $n = 1$, 2, and 3. Only a difference of less than 10 kJ mol^{-1} can be observed when relaxation of geometry in a continuum is considered. PCM calculations using both sets of geometries also indicate a similar trend.

Until now, the interaction between solvent and solute was described by keeping only the dipole moment of the solute (SCRF(μ)). An improved approximation includes the quadrupole moment of the solute (SCRF(Q)). As shown in Table 8, the quadrupole terms lower the considered energy barriers by only a few kJ mol^{-1} and do not seem to play a significant role.

TABLE 6: Total (hartree) and Relative (kJ mol^{-1}) Energies of the Considered Stationary Points Including a Solvent Continuum ($\epsilon = 78.3$), Using SCRF and PCM Methods

	MP2/SCRF[a] 6−31g**	MP2/SCRF[a] 6−311++g**	MP2/SCRF[b] 6−311++G**	MP2/PCM[c] 6−31G**
		Total Energies		
CO_2	−188.107 74	−188.206 28	−188.203 63	−188.110 37
H_2O	−76.223 20	−76.278 62	−76.278 44	−76.230 49
$CO_2 + H_2O$	−264.330 94	−264.484 90	−264.482 07	−264.340 86
$CO_2\cdots H_2O$ **R1**	−264.334 88	−264.487 38	−264.485 77	−264.344 93
TS **TS1**	−264.254 86	−264.400 79	−264.397 09	−264.262 11
H_2CO_3 **P1**	−264.322 08	−264.467 88	−264.465 46	−264.337 10
$CO_2 + 2H_2O$	−340.554 14	−340.763 52	−340.760 51	−340.571 35
$CO_2\cdots 2H_2O$ **R2**	−340.569 86	−340.773 23	−340.773 42	−340.587 80
TS **TS2**	−340.526 4	−340.721 81	−340.725 35	−340.539 05
$H_2CO_3\cdots H_2O$ **P2**	−340.569 91	−340.773 27	−340.761 67	−340.577 39
$H_2CO_3 + H_2O$	−340.545 28	−340.746 50	−340.743 90	−340.567 59
$CO_2 + 3H_2O$	−416.777 34	−417.025 12	−417.038 95	−416.801 84
$CO_2\cdots 3H_2O$ **R3**	−416.812 62	−416.065 12	−417.061 92	−416.833 87
TS **TS3**	−416.773 30	−417.020 17	−417.020 18	−416.795 66
$H_2CO_3\cdots 2H_2O$ **P3**	−416.801 18	−417.048 71	−417.058 32	−416.823 30
$H_2CO_3 + 2H_2O$	−416.768 48	−417.025 12	−417.022 34	−416.798 08
		Relative Energies[d]		
$CO_2 + H_2O$	18	15	7	8
$CO_2\cdots H_2O$ **R1**	0	0	0	0
TS **TS1**	212	229	235	219
H_2CO_3 **P1**	59	78	68	36
$CO_2 + 2H_2O$	10	82	37	30
$CO_2\cdots 2H_2O$ **R2**	0	0	0	0
TS **TS2**	114	135	126	128
$H_2CO_3\cdots H_2O$ **P2**	12	12	43	39
$H_2CO_3 + H_2O$	69	71	82	57
$CO_2 + 3H_2O$	70	82	37	61
$CO_2\cdots 3H_2O$ **R3**	0	0	0	0
TS **TS3**	107	122	114	104
$H_2CO_3\cdots 2H_2O$ **P3**	42	55	21	40
$H_2CO_3 + 2H_2O$	111	100	99	89

[a] Based on gas phase geometries at the MP2/6-31G(d,p) level. [b] Based on geometries optimized including a solvent continuum at the HF/SCRF/6-31G(d,p) level. [c] Results from PCM/ MP2/6-31G(d,p) calculations. [d] All values are corrected by zero point energies.

TABLE 7: Energy Barriers (kJ mol^{-1}) of the CO_2 Hydration in Solvent Continuum ($\epsilon = 78.3$), Using SCRF and PCM Models

	energy barriers[d]			
	MP2/SCRF[a] 6-31g**	MP2/SCRF[a] 6-311++g**	MP2/SCRF[b] 6-311++G**	MP2/PCM[c] 6-31G**
$1H_2O$	212	229	235	219
$2H_2O$	114	135	126	128
$3H_2O$	107	122	114	104

[a] Based on gas-phase geometries at the MP2/6-31G(d,p) level. [b] Based on geometries optimized including a solvent continuum at the HF/SCRF/6-31G(d,p) level. [c] Results from PCM/ MP2/6-31G(d,p) calculations. [d] All values are corrected by zero-point energies.

Solvent Effect Using a Combined Model. To combine different aspects of solvent effects, we used the direct reaction field formalism (DRF) developed by Van Duijnen and co-workers[27b] whose essential features have been implemented in the HONDRF program. Specifically, all minima and transition structures given above were surrounded by 26 water molecules and a Monte Carlo (MC) sampling was performed. The numberof MC steps was limited to 10 000 because of the extremely high CPU demands. The solute and solvent systems were in turn surrounded by a dielectric continuum ($\epsilon = 78.3$). Results listed in Table 9 show that the solvent reaction field does not change the qualitative picture described above. Accordingly, energy barriers amount now to 275 kJ mol^{-1} for $n = 1$, compared with 270 kJ mol^{-1} calculated by the SCRF method at the same level. For $n = 2$, we obtained 182 kJ mol^{-1} versus 166 kJ mol^{-1} with the previous method. The variations turn out to be rather small.

TABLE 8: Dipolar and Quadrupolar Reaction Field (SCRF) Effects[a] (kJ mol^{-1}) for the Hydration of CO_2 and a Chain of Different Number of Water Molecules at the MP2/6-311++G(d,p) Level of Theory

	dipole	quadrupole
	Total Energies	
$CO_2\cdots H_2O$ **R1**	−264.485 77	−264.490 18
TS **TS1**	−264.397 09	−264.399 11
$CO_2\cdots 2H_2O$ **R2**	−340.773 42	−340.776 02
TS **TS2**	−340.725 35	−340.729 11
$CO_2\cdots 3H_2O$ **R3**	−417.061 92	−417.062 43
TS2 **TS3**	−417.020 18	−417.022 55
	Energy Barriers	
$1H_2O$	235	237
$2H_2O$	126	123
$3H_2O$	114	109

[a] Based on geometries optimized including a solvent continuum at the HF-SCRF/6-31G(d,p) level.

Taking all effects into account, for the CO_2 hydration in solution with a three-water chain, we would estimate an energy barrier of, at most, 90−100 kJ mol^{-1} relative to the preassociation reactants complex. Along with an entropy variation ($\Delta S^{\#}$) of, at most, −40 to −50 J mol^{-1} K^{-1}, the corresponding rate constants are about a few orders of magnitude from the experimental rate constant of 2.9×10^{-2} s^{-1} (ref 4). It is really difficult if one wants to reproduce the experimental parameters because many other conditions inherent in the experiments could not be included. Nevertheless, these estimates suggest a certain reality of the preassociation mechanism and lends further support for the primordial role of the active solvent participation.

TABLE 9: Total (hartree) and Relative (kJ mol^{-1}) Energies of the Stationary Points, Both in Gas Phase and Solvent (ϵ = 78.3) Using the DRF Method

	SCF/DZP	continuum/DZP	discrete + continuum + MC/DZP
		Total Energies	
CO_2...H_2O **R1**	−263.721 01	−263.728 36	−263.994 69
TS **TS1**	−263.616 04	−263.625 75	−263.889 78
H_2CO_3 **P1**	−263.716 42	−263.727 83	−263.985 14
CO_2···$2H_2O$ **R2**	−339.777 33	−339.804 21	−340.031 23
TS **TS2**	−339.706 89	−339.725 78	−339.961 96
H_2CO_3···H_2O **P2**	−339.773 47	−339.790 54	−340.026 97
		Relative Energies	
CO_2···H_2O **R1**	0	0	0
TS1 **TS1**	276	269	275
H_2CO_3 **P1**	12	1	25
CO_2···$2H_2O$ **R2**	0	0	0
TS2 **TS2**	185	206	182
H_2CO_3···H_2O **P2**	10	15	11
		Energy Barriers	
$1H_2O$	276	269	275
$2H_2O$	185	206	182

Dehydration of Bicarbonate Ion (HCO_3^-). We take this opportunity to comment on the dehydration of the bicarbonate ion, which is actually the reverse process of the CO_2 hydration. The spontaneous dehydration mechanism has been investigated experimentally by different workers.[4,5] In particular O'Leary[5] suggested, on the basis of the solvent isotropic effect [$k(^{12}C)/k(^{13}C)$], that the dehydration is stepwise rather than concerted. Accordingly, the first step is the protonation of the bicarbonate ion by a hydroxonium ion forming a zwitterion intermediate $H_3O^+ \cdot CO_2^-$. At the QCISD(T)/6-311++G(d,p) + ZPE level, the ($HCO_3^- + H_3O^+$) moiety lies about 680 kJ mol^{-1} higher in energy than the ($CO_2 + 2H_2O$) system (values in vacuum). Owing to such a large energy difference, the ($HCO_3^- + H_3O^+$) system goes downhill, undergoing a spontaneous proton transfer either in the gas phase or in solution, to the complex **P2** between carbonic acid and one water molecule, whose stability is reasonable (about −40 kJ mol^{-1} in vacuum and −20 kJ mol^{-1} in aqueous solution, relative to the seperated species). From the complex **P2**, a dehydration could occur passing through **TS2** giving CO_2 in the complex form **R2**. Thus, our results support the proposal that the bicarbonate dehydration is stepwise, but the identity of the relevant intermediate differs somewhat. It should, however, be stressed that the theoretical methods we use here do not allow for an adequate treatment of zwitterionic species in solution.

Concluding Remarks

The results obtained in the present theoretical study support further the view that a solvent is not only the medium in which a reaction is carried out but is also actively involved in the chemical process. Therefore, the study of a process in solution cannot always be simply related to the one taking place in the gas-phase plus nonspecific interaction with the solvent continuum; its geometrical and energy characteristics are expected to be altered fundamentally by the involvement of the solvent in the reactants and transition states. The use of the supermolecule model, with a discrete representation of the solvent, shows that the motion of the solvent molecules themselves constitutes an important part of the motion of the whole reacting system along the reaction coordinate. Regarding the neutral hydration, it proceeds via a preassociative, cooperative, cyclic, and hydrogen-transfer relay mechanism in which multiple additional water molecules provide the necessary catalytic pattern, even in the gaseous phase.

Water-catalyzed hydration of CO_2 involves simultaneously a nucleophilic attack of water oxygen on the CO_2 carbon and a more complex transfer relay of a water hydrogen atom to a CO_2 oxygen via a chain of water molecules bridging both reacting centers; the latter leads to a ring-shaped transition state and acts as both acid and base. The decrease in energy barrier associated with the simplest cooperativity and bifunctional catalysis exerted by one water molecule turns out to be the most important, the change in going from $n = 1$ to 2 being 74 kJ mol^{-1} in the gas phase and 109 kJ mol^{-1} in aqueous solution. A third water molecule (from $n = 2$ to 3) decreases the energy barrier by an additional 11 kJ mol^{-1} in the gas phase and 12 kJ mol^{-1} in water solvent. When the number of water molecules that make up the chain is increased, the energy barrier decreases, but only a small change can be observed in going from $n = 3 \rightarrow 4$ in the gas phase. In addition, in the liquid phase, no transition state containing four active water molecules in the supermolecule could be found by using a spheric SCRF model. Based on the trends in calculated activation energies, it can be concluded that the neutral hydration of CO_2 is likely to proceed via a cooperative and concerted mechanism involving active participation of three additional molecules in the gas phase or in solution containing little water and at least two additional water molecules in aqueous solution. Electrostatic solvent effects seem to be another stabilizing factor for the highly polarized water-chained transition structures, but overall, the hydration of CO_2 no doubt constitutes another case of active solvent catalysis where the solvent molecules fully participate as a catalyst in the chemical transformation.

On the basis of all these trends, it can be concluded that the neutral hydration of CO_2 proceeds via a water chain mechanism involving the active participation of three water molecules ($n = 3$) in neutral aqueous solution and four water molecules ($n = 4$) in the gaseous phase.

Acknowledgment. The authors are grateful to the Flemish Science Organizations (FWO, IWT, and GOA) and the KU Leuven and RU Groningen Computing Centers for continuing support.

References and Notes

(1) Zelitch, I. *Annu. Rev. Biochem.* **1975**, *44*, 923 and references therein.
(2) Mills, G. A.; Urey, H. C. *J. Am. Chem. Soc.* **1940**, *62*, 1019.
(3) Magid, E.; Turbeck, B. O. *Biochim. Biophys. Biophys. Acta* **1968**, *165*, 515.
(4) Pocker, Y.; Bjorkquist, D. W. *J. Am. Chem. Soc.* **1977**, *99*, 6537.
(5) Marlier, J. F.; O'Leavy, M. H. *J. Am. Chem. Soc.* **1984**, *156*, 5054.
(6) Terlow, J. K.; Lebrilla, C. B.; Schwarz, H. *Angew. Chem.* **1987**, *99*, 352.
(7) Rasul, G.; Reddy, V. P.; Zdunek, L. Z.; Prakash, G. K. S.; Olah, G. *J. Am. Chem. Soc.* **1993**, *115*, 2236.
(8) (a) Hage, W.; Hallbrucker, A.; Mayer, E. *J. Am. Chem. Soc.* **1993**, *115*, 8427. (b) Moore, M. H.; Khanna, R. K. *Spectrochim. Acta* **1991**, *477*, 255.
(9) Wight, C. A.; Boldyrev, A. I. *J. Phys. Chem.* **1995**, *99*, 12125.
(10) Radom, L.; Lathan, W. A.; Hehre, W. J.; Pople, J. A. *Aust. J. Chem.* **1972**, *25*, 1601.
(11) (a) Jönsson, B.; Karlström, G.; Wenerström, H.; Roos, B. *Chem Phys. Lett.* **1976**, *41*, 317. (b) Jönsson, B.; Karlström, G.; Wenerström, H.; Fosen, S.; Roos, B.; Almlof, J. *J. Am. Chem. Soc.* **1977**, *99*, 4628.
(12) (a) Williams, J. O.; Van Alsenoy, C.; Schäfer, L. *J. Mol. Struct.: THEOCHEM* **1981**, *76*, 109. (b) Schäfer, L.; Van Alsenoy, C.; Scarsdale, J. N.; Sellers, H. L.; Pinegar, J. J. *J. Mol. Struct.: THEOCHEM* **1982**, *86*, 267.
(13) (a) Sokalski, W. A. *Int. J. Quantum Chem.* **1981**, *20*, 231. (b) Sokalski, W. A. *J. Mol. Struct.* **1986**, *138*, 77.
(14) George, P.; Bock, C. W.; Trachtman, M. *J. Comput. Chem.* **1982**, *3*, 283.
(15) Jean, Y.; Volatron, F. *Chem. Phys.* **1982**, *65*, 107.
(16) Nguyen, M. T.; Ha, T.-K. *J. Am. Chem. Soc.* **1984**, *106*, 599.
(17) Liang, J.-Y.; Lipscomb, W. N. *J. Am. Chem. Soc.* **1986**, *108*, 5051.

(18) Buckingham, A. D.; Handy, N. C.; Rice, J. E.; Somasundram, K.; Dijkgraaf, C. *J. Comput. Chem.* **1986**, *7*, 283.
(19) Nguyen, M. T.; Hegarty, A. F.; Ha, T.-K. *J. Mol. Struct.* **1987**, *150*, 319.
(20) Merz, K. M., Jr. *J. Am. Chem. Soc*. **1990**, *112*, 7973.
(21) Tachibana, A.; Fueno, H.; Tanaka, E.; Murashima, M.; Koizumi, M.; Yamabe, T. *Int. J. Quantum Chem.* **1991**, *39*, 561.
(22) Nguyen, M. T.; Hegarty, A. F. *J. Am. Chem. Soc*. **1983**, *105*, 3811.
(23) Nguyen, M. T.; Hegarty, A. F. *J. Am. Chem. Soc*. **1984**, *106*, 1552.
(24) (a) Raushel, F. M.; Villafranca, J. J. *J. Am. Chem. Soc*. **1980**, *102*, 6619. (b) Williams, I. H.; Spangler, O.; Femec, D. A.; Maggiora, G. M.; Schowen, R. L. *J. Am. Chem. Soc*. **1983**, *105*, 31. (c) Ventura, O. N.; Coitino, E. L.; Lledós, A.; Bertran, J. *J. Comput. Chem*. **1992**, *13*, 1037.
(25) Wolfe, S.; Kim, C.-K.; Yang, K.; Weinberg, N.; Shi, Z. *J. Am. Chem. Soc*. **1995**, *117*, 4240.
(26) Frisch, M. J.; Trucks, G. W.; Schlegel, H. B.; Gill, P. M. W; Johnson, B. G.; Robb, M. A.; Cheeseman, J. R.; Keith, T.; Petersson, G. A.; Montgomery, J. A.; Raghavachari, K.; Al-Laham, M. A.; Zakrzewski, V. G.; Ortiz, J. V.; Foresman, J. B.; Cioslowki, J.; Stefanov, B. B.; Nanayakkara, A.; Challacombe, M.; Peng, C. Y.; Ayala, P. H.; Chen, W.; Wong, M. W.; Andres, J. L.; Replogle, E. S.; Comperts, R.; Martin, R. L.; Fox, D. J.; Binkley, J. S.; DeFrees, D.J.; Baker, J.; Stewart, J. J. P.; Head-Gordon, M.; Gonzalez, C.; Pople, J. A. *GAUSSIAN 94*, Revision C.3; Gaussian Inc.: Pittsburgh, PA, 1995.
(27) (a) Miertus, S.; Scrocco, E.; Tomasi, J. *Chem. Phys.* **1981**, *55*, 117. (b) De Vries, A. H.; Van Duijnen, P. Th.; Juffer, A. H. *Int. J. Quantum Chem. Symp*. **1993**, *27*, 451. De Vries, A. H.; Van Duijnen, P. Th.; Juffer, A. H.; Rullmann, J. A. C.; Dijkman, J. P.; Merenga, H.; Thole, B. T. *J. Comput. Chem*. **1995**, *16*, 37.
(28) Coan, C. R.; King, A. D. *J. Am. Chem. Soc.* **1971**, *93*, 1857.
(29) Fredlin, L.; Nelande, B.; Ribbegard, G. *Chem. Scr*. **1975**, *7*, 11.
(30) Tso, T. L.; Lee, E. K. *J. Phys. Chem.* **1985**, *89*, 1612, 1618.
(31) Falk, M.; Miller, A. G. *Vib. Spectrosc.* **1992**, *4*, 165.
(32) Peterson, K. I.; Klemperer, W. *J. Chem. Phys.* **1984**, *80*, 3439.
(33) Makarewicz, J.; Ha, T. K.; Bauder, A. *J. Chem. Phys.* **1993**, *99*, 3694.
(34) Koehler, J. E. H; Saenger, W. *J.Comput. Chem*. **1987**, *8*, 1090.
(35) Gandour, R. D. *Tetrahedron Lett*. **1974**, 295−298.